Evaluation of Injection-Molding Simulation Tools to Model the Cure Kinetics of Rubbers

A. Arrillaga,[1] A. M. Zaldua,[1] A. S. Farid[2]

[1]*Materials Department, Lea-Artibai Ikastetxea S. Coop., Xemein Etorbidea 19, Markina-Xemein 48270, Vizcaya, Spain*
[2]*London Metropolitan Polymer Centre, London Metropolitan University, 166-220 Holloway Road, London N7 8DC, United Kingdom*

Received 23 June 2010; accepted 1 December 2010
DOI 10.1002/app.33880
Published online 16 August 2011 in Wiley Online Library (wileyonlinelibrary.com).

ABSTRACT: Rubber injection molding is a process whereby a rubber mix is injected into a closed mold where the material is shaped to the desired geometry. Having completely filled the cavity rubber mix is vulcanized. Vulcanization is the process whereby a viscous and tacky uncured rubber is converted into an elastic material through the incorporation of chemical crosslinks between the polymer chains. The degree of cure achieved depends on the formulation recipe and the time–temperature history endured by the material during the curing process while in the mold. The aim of this study was to check the capability of commercial injection-molding simulation tools, such as Moldflow and Cadmould, to predict the degree of cure achieved in spiral-shaped parts when subjected to various cure cycles. To use the simulation tools, it was necessary to characterize the material in terms of their thermal properties and kinetic behavior during curing. The degrees of cure were determined with swelling techniques and by the measurement of the residual cure exotherms with differential scanning calorimetry. On comparing the experimental values of the degree of cure with those predicted by the simulation tools, we found that the initial simulations underestimated the degrees of cure. Consequently, the criteria used to calculate the cure model parameters were modified to invoke faster cures. In so doing, good agreement was achieved between the degrees of cure predicted by the simulations and those obtained experimentally.© 2011 Wiley Periodicals, Inc. J Appl Polym Sci 123: 1437–1454, 2012

Key words: crosslinking; injection molding; rubber; vulcanization

INTRODUCTION

The injection molding of rubber began in the early 1940s. Today, the process is used for manufacturing a wide range of industrial products. Essentially, a rubber mix is placed inside an injection unit and subsequently injected into a closed mold, which allows the rubber to take the shape of the cavity. The material parameters that define the mold-filling process are based on the thermal and rheological properties.[1]

When the cavity is filled, temperature gradients persist in the rubber; this results in temperature distributions within the bulk of the rubber. Material residing at the end zone of the filling section is subjected to an extensive heating regime during the mold-filling stage, and therefore, the material in this region is at a higher temperature than the material near the gate. As the mold is set at a high temperature, the material continues heating because of convection and begins to cure when a certain critical temperature is achieved. This temperature depends on the curing system used in the formulation recipe. Each material zone suffers a different time–temperature history; this leads to a distribution of cure levels. The degree of cure achieved depends on the main process parameters:

- The temperature of the material when the mold is completely filled.
- The temperature of the mold cavity.
- The time for which the material is kept in the mold, that is, the cure time.

To simulate the cure process, it is necessary to characterize the materials in terms of their thermal and curing properties. Recently, various authors[2] have discussed the various techniques that are available to characterize cure behavior.

In this study, spiral-shaped rubber parts were injected and subsequently cured in a mold for different cure times so as to produce a series of molded spiral parts having various levels of cure. Studies were carried out with two rubber formulations with a common peroxide cure vulcanization system. One formulation was based on Acrylonitrile-Budadiene-Rubber (NBR), and the second was based on Ethylene-Propylene-Diene Rubber (EPDM). The degree of cure achieved at two specific locations in the molded parts was evaluated with two swelling techniques[3,4]

Correspondence to: A. Arrillaga (aarrillaga@leartik.com).
Contract grant sponsors: Lea Artibai Ikastetxea S. Coop, Azaro Fundazioa, European foundation for regional development (FEDER), Basque Country Government.

TABLE I
Recipe for the NBR and EPDM Formulations

NBR		EPDM	
NBR rubber Europrene N3345	100 phr	EPDM rubber Nordel IP 4570	50 phr
Carbon black N-330	60 phr	EPDM rubber Nordel IP 4520	50 phr
Dioctyl phthalate	10 phr	Carbon black FEF N-539	35 phr
Stearic acid	1 phr	Parafinic oil	15 phr
Zinc oxide	5 phr	Zinc oxide	5 phr
Dicumyl peroxide Percadox BC-40MB	6.5 phr	Dicumyl peroxide Percadox BC-40MB	10 phr

and also with differential scanning calorimetry (DSC) to measure residual heat. It's the commercial name of the tool were used to model this process: Moldflow Plastics Insight (MPI) Reactive Molding and Cadmould's 3D-F. Both are Finite Element Modelling (FEM)[5] based tools in which the geometry is represented with a mesh. Once the behavior of the material is characterized, the appropriate governing equations are invoked; this allows the degree of cure to be determined. Values obtained in this way were found to fall below the experimental values. To circumvent this disparity, the model was adjusted to give faster cures by the use of a criterion that was based on the application of a lower temperature when the data were fit to the induction and cure models. Application of this methodology gave results that showed good agreement with those determined experimentally.

EXPERIMENTAL

Materials

Two rubber compounds were studied. Both were peroxide-cured formulations, one based on EPDM and the other based on NBR. Table I summarizes the recipe of the NBR and EPDM compounds. Batches of about 57 kg were prepared by Elastorsa S.A. Co. (Arnedo, Spain) in a 70-L internal mixer.

Material characterization

Even though the interest of this work was the study of the curing phase, for simulation purposes, it was necessary to characterize the material in terms of its rheology, thermal properties, and curing.

Rheology characterization

A Rosand RH 2.2 rheometer (Malvern Instruments Ltd, Worcestershire, England) was used for test purposes. Capillaries 2 mm in diameter with lengths of 8, 12, 16, and 25 mm were selected. Ram speeds in the range 0.25–500 mm/s were used. The apparent viscosity data versus the apparent (uncorrected) shear rate data were calculated for temperatures of 80, 90, 100, and 110°C. The correction of Bagley[6,7] and Rabinowitsch[8] were applied to calculate the corrected viscosity data. These data were used to define the rheology model. The material supplied from the batch manufacturer was passed trough the injection unit at the same process conditions as those used during the further injection trials, and capillary measurements were made on this material.

Moldflow is based on the reactive viscosity model:[9]

$$\eta = \frac{\eta_0(T)}{1 + \left[\frac{\eta_0(T)\dot{\gamma}}{\tau^*}\right]^{(1-n)}} \times \left(\frac{\alpha_g}{\alpha_g - \alpha}\right)^{C_1 + C_2\alpha} \quad (1)$$

$$\eta_0 = B \exp(T_b/T) \quad (2)$$

where η is viscosity, η_0 is zero viscosity, γ is the shear rate, τ^* represents the stress level at the transition between newtonian and power law regions, α_g is the degree of curve at gelation point, C_1 and C_2 are fitting parameters, B and T_b are fitting parameters, T is the temperature. The terms C_1 and C_2 were set to 1 and 0 on the basis that the rubbers used in this work did not cure during the filling phase. α is the degree of cure, and the gelation conversion (α_g) was set to 0.1 as a default value. The parameters τ^*, n, B, and T_b were calculated with Grace software.[10] The procedure used to determine the model parameters was the same as that used recently.[1] Table II indicates the values obtained for both formulations.

Rheology was defined through the combined Carreau[11] and William Landel Ferry (WLF)[12] model for Cadmould:

$$\eta(\dot{\gamma}, T) = \frac{P_1 a_T}{(1 + a_T \dot{\gamma} P_2)^{P_3}} \quad (3)$$

$$\text{Log } a_T = \frac{8.86|T_0 - T_s|}{101.6 + T_0 - T_s} - \frac{8.86|T - T_s|}{101.6 + T - T_s} \quad (4)$$

where P1 indicates the "Zero viscostity", that is, viscosity at low shear rates. P2 indicates the value of shear stress at the transition point between the newtonian and

TABLE II
Parameters of the Reactive Viscosity Model for NBR and EPDM

NBR	NBR	EPDM
τ^* (Pa)	135,360	128,450
n	0.21509	0.06857
B (Pa.s)	0.0007471	0.00062
T_b (K)	7300.8	9871.1
C_1	1	1
C_2	0	0
α_g	0.1	0.1

TABLE III
Parameters of the Carreau + William Landel Ferry (WLF) Viscosity Model for NBR and EPDM

	NBR	EPDM
P_1 (Pa s)	19046	20209
P_2 (s)	0.080145	0.10053
P_3	0.78491	0.899
P_4 (Pa s)	0	0
T_0 (°C)	110	110
T_s (°C)	−262.90	−425.24

pseudoplasticity region. P3 indicates the power law index. a_T is the shift factor. T_0 is the reference temperature for WLF superposition and Ts is fitting parameter. After selecting a reference temperature (T_0) of 110°C, which was the closest temperature to the real temperature at which materials entered the mold, we fit the viscosity data to the first expression using KGraph software,[13] and values for P_1, P_2, and P_3 were calculated. Considering the shift between viscosity curves at different temperatures, we defined a_T, and according the second expression, the value of T_s was calculated. Table III summarizes the values obtained for both formulations.

Thermal measurements

For the application of Moldflow, the thermal properties required are specific heat (C_p) and thermal conductivity (K), whereas Cadmould requires knowledge of K and the thermal diffusivity (Fi).

Although several methods can be found in the literature to measure C_p,[14–16] measurements were made with a TA Q100 DSC device (TA Instruments, New Castle, De, USA) in the range from 70 to 215°C with a scan rate of 20°C/min. The dependency with temperature was studied. The values obtained ranged from 1.54 to 1.83 J g^{-1} $(°C)^{-1}$ for NBR and from 1.84 to 2.24 J g^{-1} $(°C)^{-1}$ for EPDM. The variation with degree of cure was neglected. Measurements were made on completely cured samples.

K also varied both with the temperature and degree of cure. The variation with degree of cure was not considered. To measure K accurately, specific apparatus are required. ASTM F433-02 and DIN 52612 describe standard procedures for measuring K. The most common techniques are the hot-line/hot-wire method,[17–20] Guarded hot-plate method[17,21–23] (ASTM C177-04), Lee's disc apparatus[24–26] (ASTM C-158), hot-disc devices,[27] and DSC measurements (normally with modulated DSC[26,28–33]). In this work, a Haake pvT100 device (Thermo Fisher Scientific Inc., Waltham, MA, USA) was used, which also had the capability to perform K measurements. The dependency with temperature was studied within the ranges 0.186–0.243 W m^{-1} K^{-1} for NBR and 0.245–0.295 W m^{-1} K^{-1} for EPDM.

Thermal diffusivity may be calculated with specific techniques, such as with the List method,[34,35] a two-solvent method,[36] or some other reliable technique involving direct measurements.[37–39] In this work, values were calculated with the ratio of K to the volumetric heat capacity and density of the material ranging from 80 to 180°C. In this way, values were obtained ranging from 0.101 to 0.116 mm^2/s for NBR and 0.128 to 0.134 mm^2/s for EPDM:

$$\phi = \frac{K}{\rho C_p} \tag{5}$$

where ϕ is the thermal diffusivity and ρ is the density of the rubber formulation.

Curing measurements

In the literature, several useful techniques have been described for characterizing the curing process of elastomers; these include Moving Die Rheometer (MDR), DSC, Oscillating Disc Rheometer (ODR), Fourier transform infrared spectroscopy, dynamic mechanical thermal analysis, and equilibrium swelling.[40–44] From such techniques, a parameter known as the *degree of cure* is defined, which is subsequently plotted against time to give a useful representation of the way in which the extent of cure varies with the passage of time.

Recently, we[2] presented and discussed the application and utility of three different techniques for characterizing the cure behavior of rubber compounds. These included the use of MDR, ODR, and DSC. Among these, for this study, MDR and DSC measurements were considered.

MDR tests. An MDR 2000 from Alpha Technologies was used. Tests were made according to the ASTM D 5289 procedure at test temperatures of 150, 160, 170, and 180°C. The elastic torque signal (S') versus time was used for defining both the induction and the kinetics of curing. The *induction time* is defined as the time at which the torque decreases to the point of minimum torque (point A), as described in Figure 1. With respect to the cure, in this study, point A was considered to be the initial point at which time and α (degree of cure) were zero. In the absence of marching modulus, the cure is said to be complete (100 % of cure) on the attainment of a plateau region (point B). At point B, the torque reaches the maximum value, and the degree of cure is defined as the point at which $\alpha = 1$. The way in which the degree of cure (α) varied with time was determined with values of torque. The cure rate ($d\alpha/dt$) was defined in terms of the following relationships:

Determination of degree of cure :

$$\alpha_i = \frac{\text{Torque}_i - \text{Torque}_{\min}}{\text{Torque}_{\max} - \text{Torque}_{\min}} \tag{6}$$

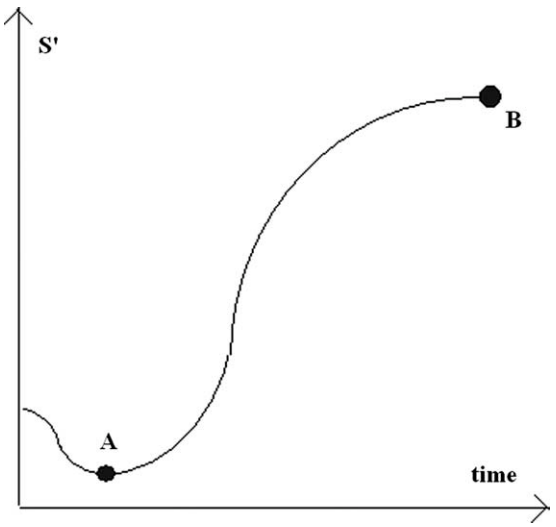

Figure 1 Example of an MDR test. Representation of the S′ shape plot generated showing the minimum and maximum torque points.

$$\text{Determination of cure rate}: \frac{d\alpha}{dt}_i = \frac{\alpha_i - \alpha_{(i-1)}}{t_i - t_{(i-1)}} \quad (7)$$

where t is the time, The subscript "i" makes reference to the data set available for a certain test time.

DSC tests. DSC measures the temperatures and heat flows associated with transitions in materials as a function of temperature or time in a controlled atmosphere. The cure process is associated with an exothermic process, so exothermity evolution is related to the level of cure. The degree of cure is assumed to be proportional to the number of bonds formed during crosslinking, and each bond releases the same amount of heat. The exotherm produced by rubbers is usually low, but Brazier and Nickel[45] showed that DSC was capable of detecting the exothermity (Q) down to very low levels.

A Q100 DSC instrument from TA Instruments was used. Isothermal tests were made at 150, 160, 170, and 180°C. This test generates a profile of dQ/dt versus time, as shown in Figure 2.

The *induction time* is defined as the time lag between the time at which the test commences and the point at which exothermity commences (point A). Cure begins at point A and ends at point B. The parameter ΔH_T is the total area under the curve up to the baseline, and ΔH_t is the heat released up to time t. The degree of cure (from 0 to 1) can be calculated with the following equation:

$$\alpha(t) = \frac{\Delta H_t}{\Delta H_T} \quad (8)$$

Data fitting: Definition of the cure models' parameters. Moldflow and Cadmould were used for simulation purposes. In both cases, the curing of the material needed to be defined in terms of the induction and cure kinetics with appropriate models. Although mechanistic kinetics models have been developed and described in the literature,[42,43,46–49] the use of phenomenological or empirical models is more common, as is the case with both simulation tools.

Moldflow defined the induction sequence using an Arrhenius type dependence,[50] where curing was defined with the Kamal–Sourour[51] model. Data measured from MDR and DSC tests were fitted to these models with KGraph[13] software. Table IV summarizes the parameter values calculated for both formulations.

$$\text{Induction}: t_i(T) = B_1 \exp^{(B_2/T_0)} \quad (9)$$

$$\text{Cure kinetics}: \frac{d\alpha}{dt} = (K_1 + K_2\alpha^m)(1-\alpha)^n \quad (10)$$

$$K_1 = A_1 \exp\left(-E_1/RT\right) \text{ and } K_2 = A_2 \exp\left(-E_2/RT\right) \quad (11)$$

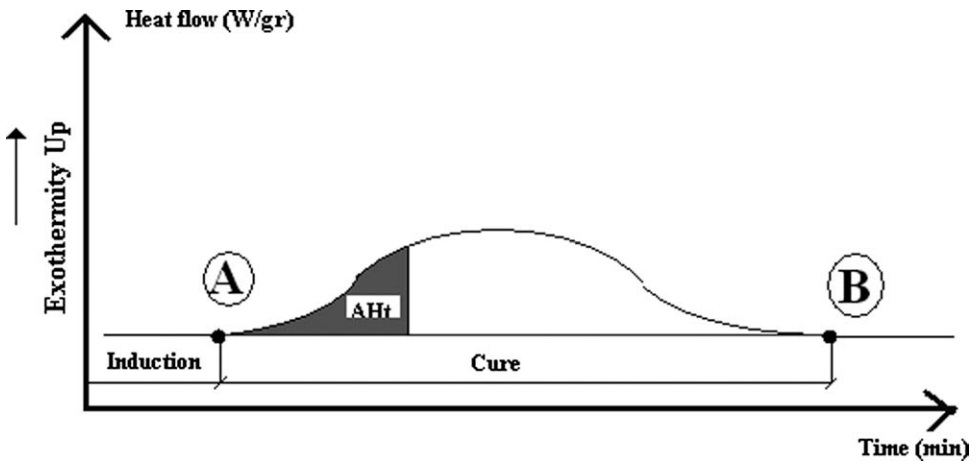

Figure 2 Heat flow release during material cure in an isothermal test.

TABLE IV
Cure Parameters Defined for the NBR and EPDM Formulations for Moldflow

Material	NBR		EPDM	
Cure kinetics technique	MDR	DSC	MDR	DSC
B_1 (s)	0.0036978	4.93×10^{-12}	0.0007165	0.00094200
B_2 (K)	3,591	12,425	4,397.5	4,258.8
A_1 (s^{-1})	0	0	0	0
E_1/R (K)	0	0	0	0
A_2 (s^{-1})	1.97×10^{15}	1.84×10^{14}	3.01×10^{15}	1.39×10^{12}
E_2/R (K)	17,365	16,323	17,704	14,260
m	0.42323	0.47297	0.31913	0.47909
N	1.5768	1.527	1.6809	1.857

R, Gas Universal Constant parameter, with a value of 8.31 J(mol.K).

where $t_i(T)$ is the induction time as a function of temperature and B_1 and B_2 are fitting parameters for the induction model. K_1 and K_2 are functions of the temperature and are defined by the m, n, E_1, and E_2 parameters. m and n are reaction orders; E1 and E2 are the activation energies.

Cadmould also uses an Arrhenius-type dependence[50] for induction, whereas the cure process is defined with the Isayev–Deng[52,53] model. Again, data measured from MDR and DSC tests were fitted to the these models with KGraph software;[13] Table V abridges the values for the different parameters:

$$t_i(T) = t_0 \exp(T_0/T) \quad \text{or} \quad \text{Ln}\, t_i = \text{Ln}\, t_0 + T_0/T \tag{12}$$

$$\alpha = \frac{Kt^n}{1 + Kt^n};\ K(T) = K_0 e^{(-E_0/RT)} \tag{13}$$

where $t_i(T)$ is the induction time as a function of temperature and t_0 and T_0 are time and temperature fitting parameters. n is the reaction order, and K is defined as a function of K_0 and E_0; K_0 is the cure rate parameter value, of a certain temperature and E_0 is the activation energy value.

Part design: Definition of the mold and injection machine

Injection trials were made on a spiral-shaped part. This part had a constant thickness of 6 mm, a width of 20 mm and a length of 1150 mm. A sprue was included in the part design to introduce the material emerging from the injection die into the spiral. It was the same part design as used by recent authors[1] for mold-filling studies. Figure 3 illustrates the complete injection shoot. A REP (Corbas, France) V37 vertical injection machine was used for injecting the rubber compounds.

Definition of injection trials

Injection trials were carried out according to the process parameters defined in Table VI. As indicated, cure time was set as a variable parameter because the parts were manufactured for different cure times in the range 10–480 s for NBR and 30–480 s for EPDM.

Even though temperatures were set for the screw unit and for the chamber, the temperature at which the material entered the mold became much higher than the set values. For this reason, Karam[41] proposed that shoots be injected directly into air instead of a mold and that their temperatures be measured with a temperature transducer. As described recently,[1] an REP injection unit leads to variations of temperature along the injection shoot, but an average temperature was measured and considered for subsequent work. The use of infrared measurements and the measurement through a transducer located in the injection nozzle were considered inappropriate because of their poor resolution.[41]

In a similar way, although the mold temperatures were set to 180°C, this temperature was the one measured by the transducers located inside the iron block of the mold. Thus, the real mold surface

TABLE V
Cure Parameters Defined for the NBR and EPDM Formulations for Cadmould

	NBR		EPDM	
	MDR	DSC	MDR	DSC
Induction				
$\text{Log}_{10}\, t_0$(min)	−4.21018	−13.09876	−4.92273	−4.80416
T_0 (K)	3,591	12,425	4,397.5	4,258.8
Cure kinetics				
$\text{Log}_{10}\, K_0$ (1 min^{-1} n^{-1})	29.3613	28.8719	23.2265	20.9408
E_0 (J/mol)	252,219.51	250,215.72	200,377.20	182,012.11
n	1.7344	1.8975	1.4731	1.5923

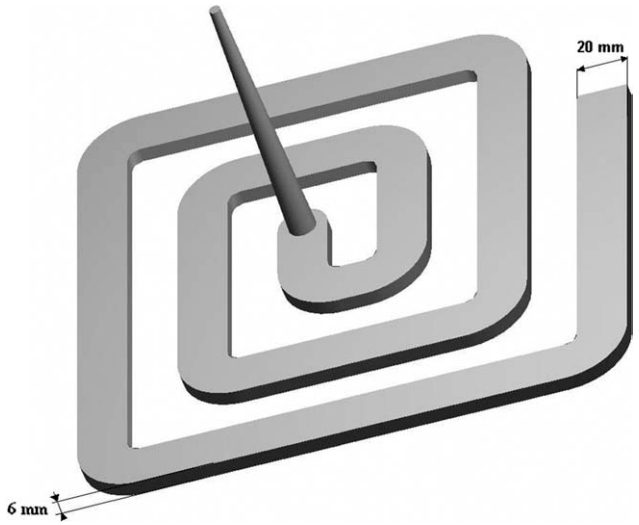

Figure 3 Representation of the complete injection shoot (mold cavity).

temperatures did not match these values. After the injection-molding cycle was completed, the real cavity surface temperature was measured with a transducer.

The average injection and mold temperatures measured during the injection trials are given in Table VII. These were the temperature values used to represent injection temperature and mold surface temperature in the injection simulations.

Simulation tools: Cadmould and Moldflow

Simulations were carried out with Moldflow's Reactive Molding and Cadmould's 3D-F tools. For Moldflow, the geometry was represented with midplane-type mesh for the spiral section (4 mm size elements) and beam-type elements for the sprue. As for Cadmould, the geometry was based on a dual-domain-type mesh for the spiral section (a default sizing of 2% of the part size was applied) and beam-type elements for the sprue.

TABLE VI
Process Parameters Used for the NBR and EPMD Formulations

Parameter	Material	
	NBR	EPDM
Extruder speed (rpm)	80	80
Extruder temperature (°C)	75	75
Chamber temperature (°C)	85	85
Mold temperature up (°C)	180	180
Mold temperature down (°C)	180	180
Lineal ram speed (mm/s)	19	12
Curing time (min)	Variable	Variable

The injection and mold temperatures given in Table VII were used in the simulation. Material models were described with the parameters described previously, where the rheology model was described together with the thermal property values. As mentioned, two different cure models were described, depending on the test procedure used to define the cure curves (MDR and DSC); simulations were carried out with both possibilities.

Measurement of the degree of cure on the parts (three procedures)

Parts were manufactured for different cure times up to a maximum cure time of 480 s for both formulations. At the end of each cure, the vulcanized part was retrieved from the mold and immersed into ice water as rapidly as possible to prevent further progress of cure. Three different procedures were used to evaluate the cure levels: swelling 1, swelling 2, and DSC. Descriptions of these methods are given in the following text.

Swelling 1: Measurements with the crosslink density (DP) data and degree of cure (DR)

Toluene was considered as the most appropriate solvent to carry out swelling measurements for both rubbers. The procedure requires prior knowledge of the value of the interaction parameter (λ) for the rubber–solvent pair used. The two-solvent procedure described by Hayes[36] was employed to determine this value; we obtained values of 0.59 and 0.43 for NBR and EPDM, respectively. On the basis of the Flory–Rehner equation,[54] the procedure purposed by Blanchard and Wootton[3,4] was used to calculate the DP data and degree of cure (DR). This procedure uses the values of the solvent–polymer interaction parameter given previously and the mass values of the swollen sample at equilibrium and the dried sample. Using these values collectively, we readily determined the average molecular weight of the chains between crosslinks (M_c). DP and the degree of cure (DR) were also calculated. Clearly, for an uncured part, the DR was zero, but it was assumed that eventually, the cure reached a steady-state or plateau value as the cure progressed. DR data were used to calculate α as a function of the cure time.

TABLE VII
Average Injection and Mold Temperatures Measured during the Injection Trials

	NBR	EPDM
Mold temperature (measured)	160°C	161°C
Injection temperature (measured)	113.0°C	111.0°C

DP and DR (the degree of cure) were calculated as follows:

$$\mathrm{DP} = \frac{\rho}{M_c/N} = \frac{\rho N}{M_c} \tag{14}$$

$$\mathrm{DR} = \left(\frac{\mathrm{DP}}{2}\right) \tag{15}$$

where N is Avogadro's number. M_c was calculated as follows:

$$M_c = \frac{1+c}{1-c} \times \frac{F(V_c)}{1.03} \tag{16}$$

where c and $F(V_c)$ are defined as the intermediate parameter to calculate the final degress of cure:

$$c = \frac{1 - V_r/V_c}{1 - V_r} \tag{17}$$

$$F(V_c) = \frac{\rho v_0 \left(V_r^{1/3} - V_r/2\right)}{-\mu V_c^2 - \mathrm{Ln}(1 - V_c) - V_c} \tag{18}$$

where V_r is the polymer volume fraction in the swollen vulcanizate, μ is the rubber–solvent interaction parameter, V_o is the Molas Mass and V_c is the polymer volume fraction with the solute considered.

The degree of cure of different parts was measured at two positions located on the spiral molding: designated as A and B in Figure 4. Slices were cut from each position and introduced into the solvent. It should be noted that the degree of cure calculated in this way is an average value within the cross section, as the spiral is considerably thick (6 mm). Actually, a difference in the degree of cure between the core and the skin was to be expected because of the presence of temperature gradients during curing.

Swelling 2: Measurements using the ratio of initial mass (m_0) to the swollen mass (m_1)

In relatively simple terms, the degree of cure achieved in samples may be quantified, although somewhat crudely, by values of m_0 and m_1. The appropriate expression to use is

$$\text{Swelling}\,(\%) = \frac{m_1 - m_0}{m_1} \times 100 \tag{19}$$

The percentage swelling decreases as the cure progresses up to the point at which a plateau is reached in the cure profile. The swelling at that point is equivalent to a cure such that $\alpha = 1$. Thus, the swelling measurements provide a simple method of quantifying the level of cure. In realization of this simplicity, ODR measurements were made on both materials to obtain preliminary complete cure profiles to obtain an overall view of the cure behavior. Having obtained the full profiles of both materials, we conducted further ODR tests, but on this occasion, the ODR was halted at intervals corresponding to 10, 20, ..., and 100 % increases in torque. At each of these intervals, ODR samples were retrieved from the cavity of the ODR and rapidly quenched. For each sample retrieved in this way, the m_0 and m_1 values were measured; this, thereby, allowed their swelling ratios to be determined. By this method, the percentage swelling data may have been related to the degree of cure. Same samples were used as those used for the swelling 1 procedure.

DSC: Measurements of the residual exothermity

As explained previously, it is important to realize when one studies cure kinetics that rubbers give out heat during cure. If the sample is completely cured, the enthalpy will be zero, whereas for partially cured samples, an intermediate value will be obtained. Thus, the degree of cure of a partially cured sample can be calculated if one knows its exothermic value and the corresponding value for the uncured sample with the following relationship:

$$\text{Degree of cure} = (\Delta H_T - \Delta H_t)/\Delta H_T \tag{20}$$

where ΔH_T is the exothermity for the uncured sample and ΔH_t is the exothermity of the sample cured during time t. Measurements were made only in zones defined as A in Figure 4. Recall when swelling procedures where used, an average degree of cure was calculated for the complete cross section of the part. In contrast, for DSC tests, samples were taken from three positions across the thickness. These positions are shown in Figure 5 and are described as the core, intermediate, and skin. They were tested within the range 110–240°C at a rate of 10°C/min.

RESULTS

Measurement of the degree of cure in the parts

As mentioned, three procedures were used to evaluate the value degree of cure of the parts, two of which were based on swelling measurements and gave an average value of degree of cure across the thickness of the molded part. The third procedure was based on the measurement of residual exothermal heat of cure through the use of DSC; measurements were made at three zones across the thickness (see Fig. 5). The results are indicated in Figure 6.

Theoretically, the skin of the material should exhibit the faster cure profile, whereas the core of the material should display the lowest cure profile.

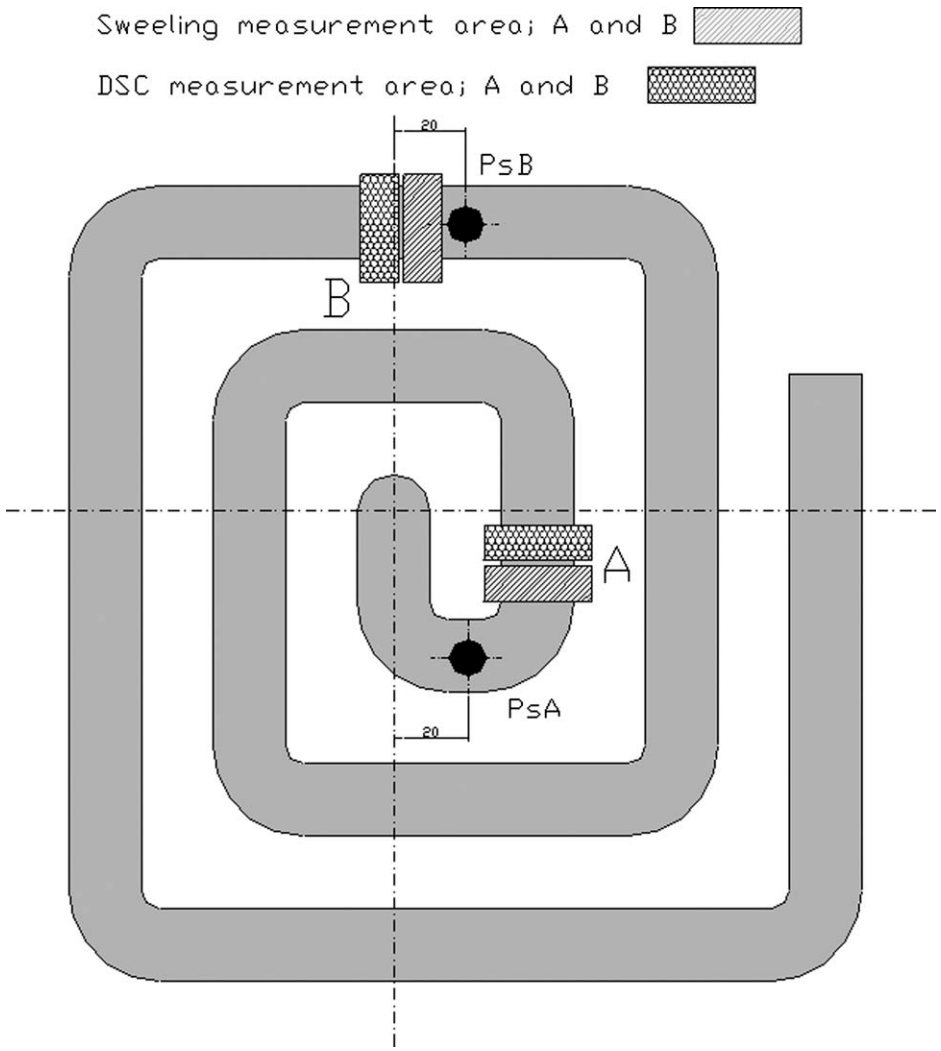

Figure 4 Diagram showing positions A and B, from which slices were cut for the determination of the degree of cure from the swelling measurements and DSC. The areas with different patterns indicate the places at which samples were taken for the swelling and DSC experiments, as indicated in the figure. P_sA and P_sB makes reference to the locations at which pressure signals were recorded during mould filling step for studies in Reference [1]

However, differences in the cure kinetics between the skin and the core were not clearly seen, and some overlap in the data was clearly observed. Such anomalies may be attributed to the poor resolution of the technique used and may well have been associated with three factors: (1) problems associated with sample preparation, (2) the low exothermity of the samples encountered, and (3) the low resolution when the exact weight of the sample was defined before the measurement. In view of such factors, a curve was produced on the basis of the average of the three DSC curves. This curve facilitated comparisons with other techniques and various simulations. Figure 7 shows the evolution of the degree of cure measured according to the procedures.

The degree of cure obtained from the procedure designated *swelling 2* progressed at a faster rate than that obtained from the procedure named *swelling 1*. The variation in the rate was attributed to differences in the calculation. One technique considered the mass of the swollen and dried sample, whereas the other took into account m_0 and m_1. The DSC results, which could only be carried out at intermediate temperatures at zone A, occupied an intermediate position between the two swelling procedures. The material in zone B cured faster than that in zone A

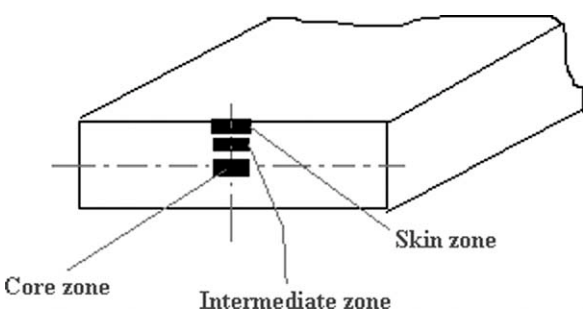

Figure 5 Diagram showing the three zones across the thickness at which the degree of cure was calculated from DSC.

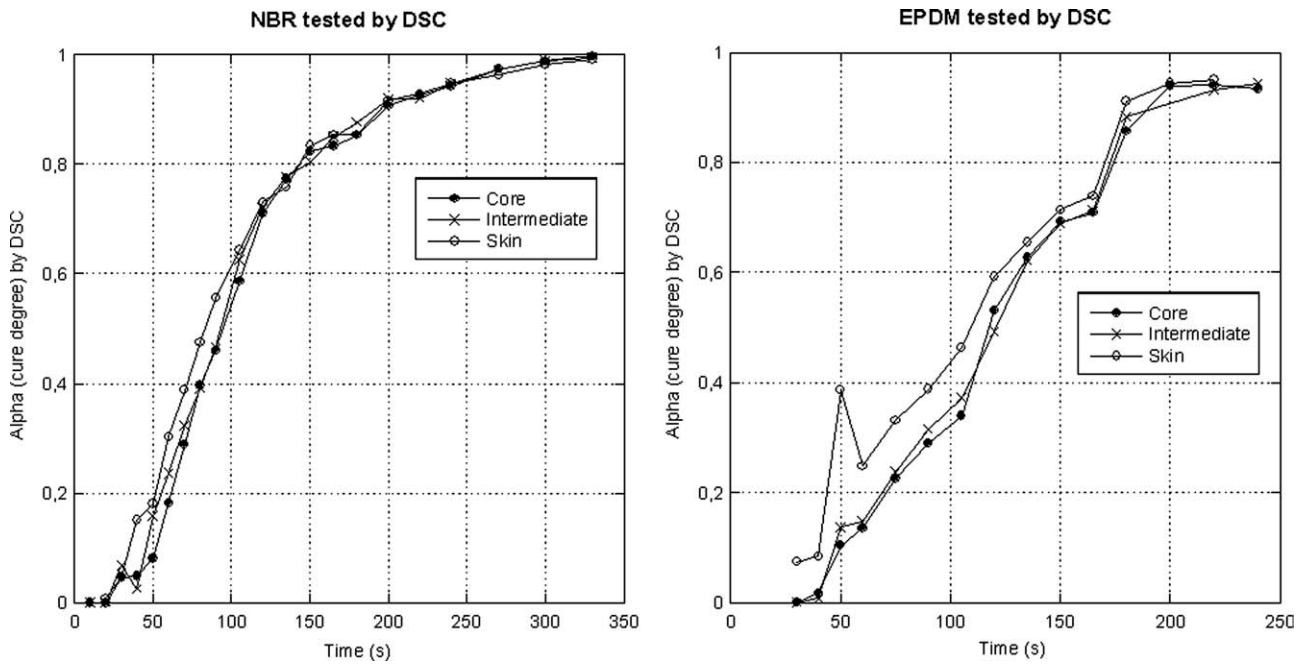

Figure 6 Definition of the cure curves measured in zone A for spiral parts injected at intermediate temperatures in NBR and EPDM.

simply because the material in zone B was at a higher temperature as compared with zone A at the end of the mold-filling phase.

Moldflow simulation results and comparison to the degree of cure measurements

Although measurements of the degree of cure showed that the parts of both materials were completely cured for a cure time of 480 s, a default cure time of 1300 s was set for Moldflow simulations. Results were available for two different cure models, depending on whether the MDR or DSC was used (see Table IV) to define the induction (scorch)[50] and cure kinetics[51] models. Results of comparisons of the experimental cure curves with those predicted by simulations with Moldflow are shown in Figures 8 and 9 for NBR and EPDM, respectively.

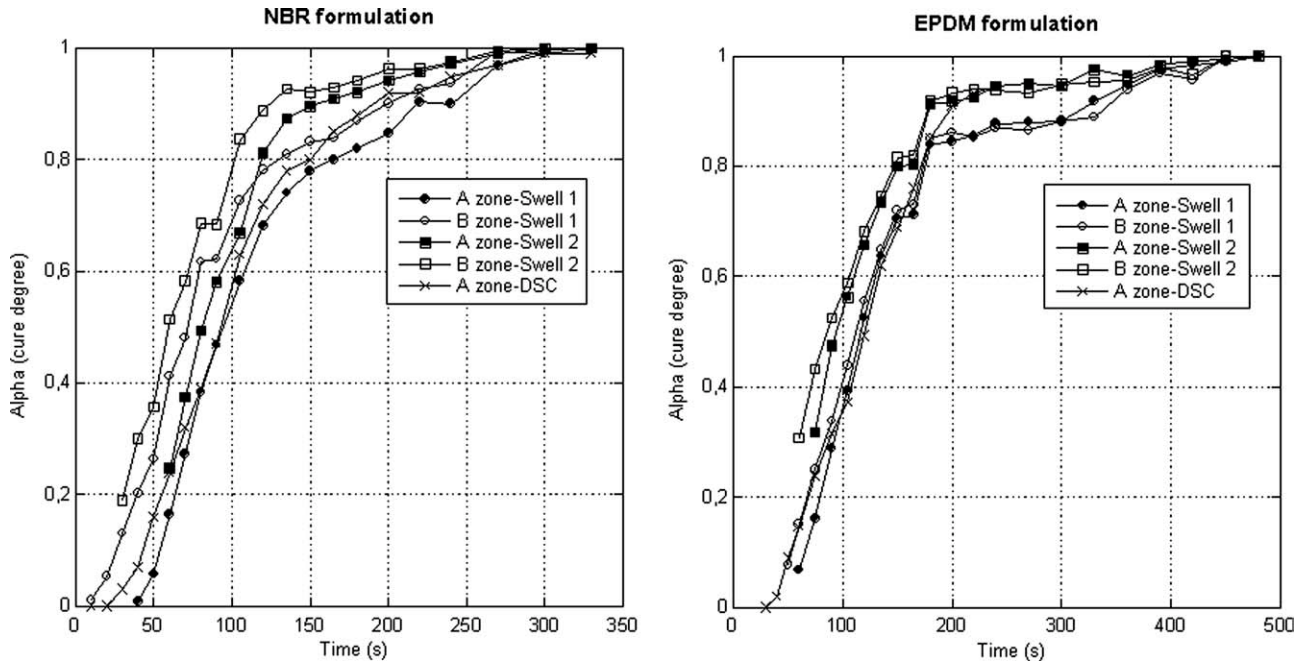

Figure 7 Cure curves calculated for NBR and EPDM according to the three test procedures.

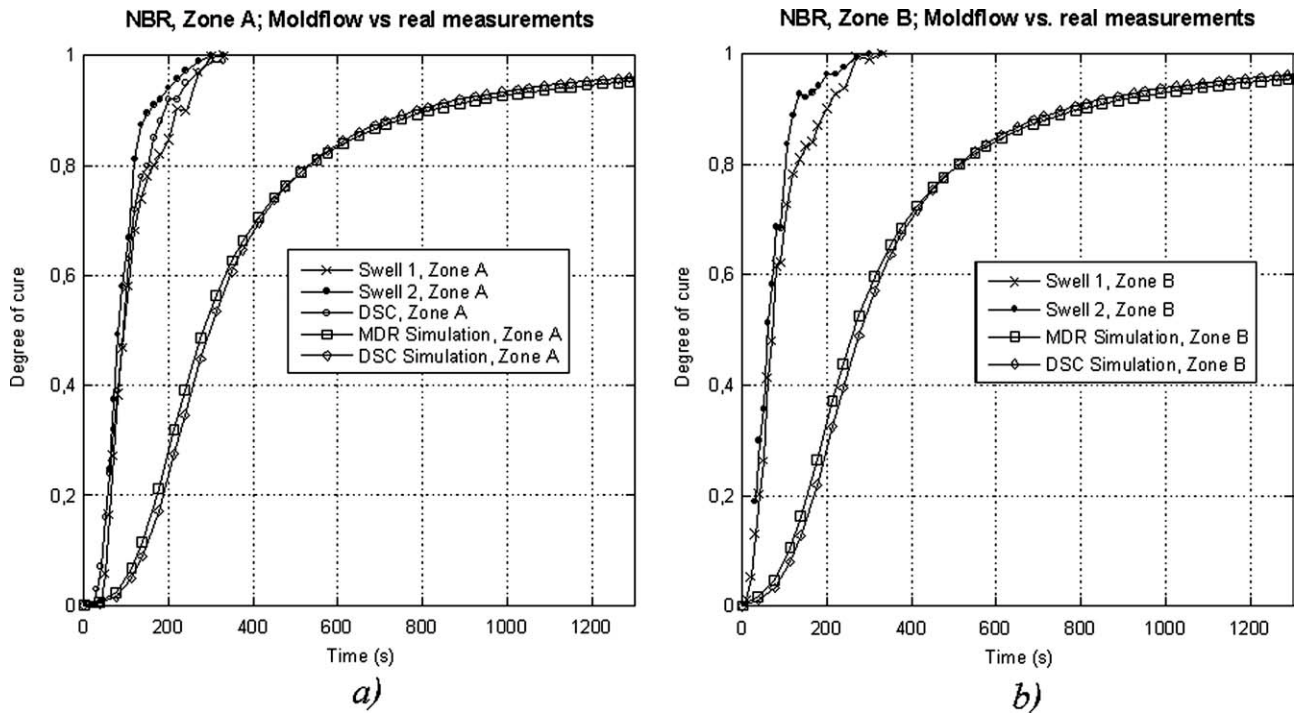

Figure 8 Comparison of the experimental and simulated (Moldflow) degrees of cure for NBR: (a) zone A and (b) zone B.

It was clearly seen that the predicted levels of cure were below those exemplified by the experimental traces. DSC and MDR gave similar results, but for EPDM, DSC traces were below those of MDR for the complete cure range. A similar pattern emerged for NBR up to degrees of cure of about 70%; above this value, the DSC data indicated a faster rate than that exemplified by DSC.

Even though lengthy cure times were used, a degree of cure of 100% was not achieved in the

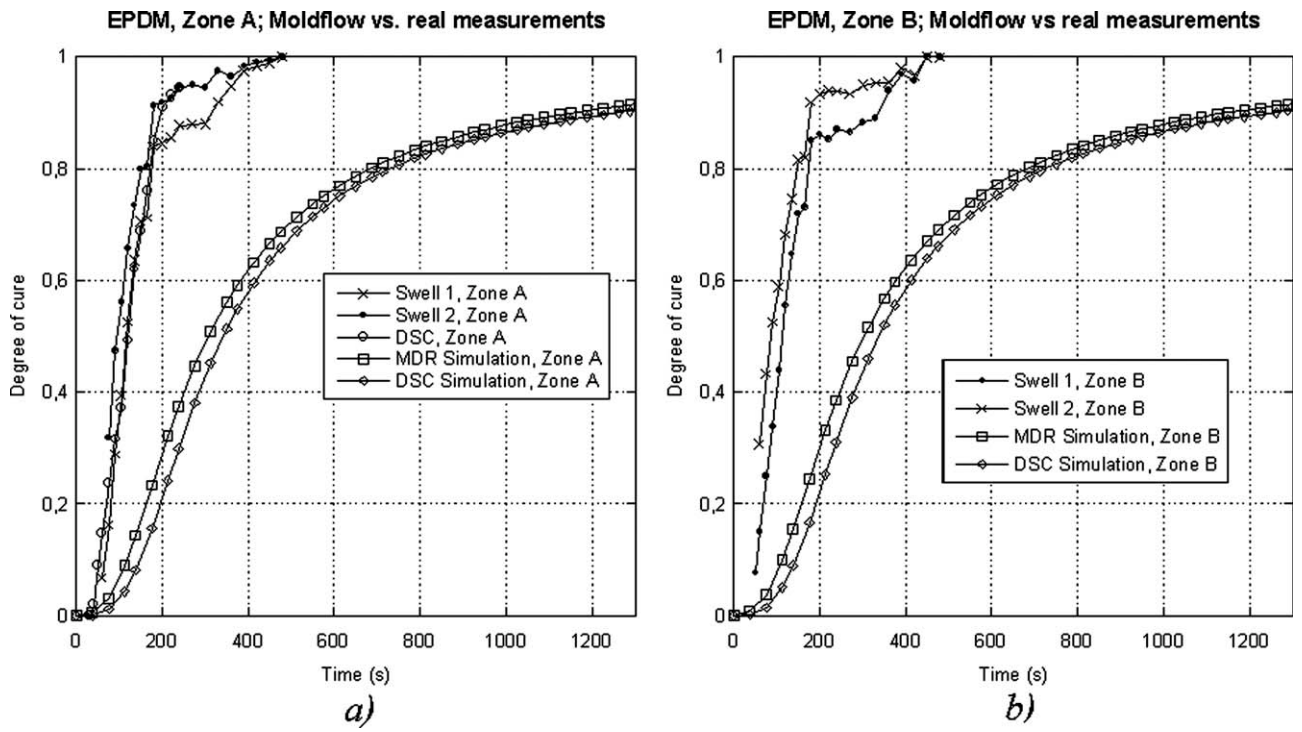

Figure 9 Comparison of the experimental and simulated (Moldflow) degrees of cure for EPDM: (a) zone A and (b) zone B.

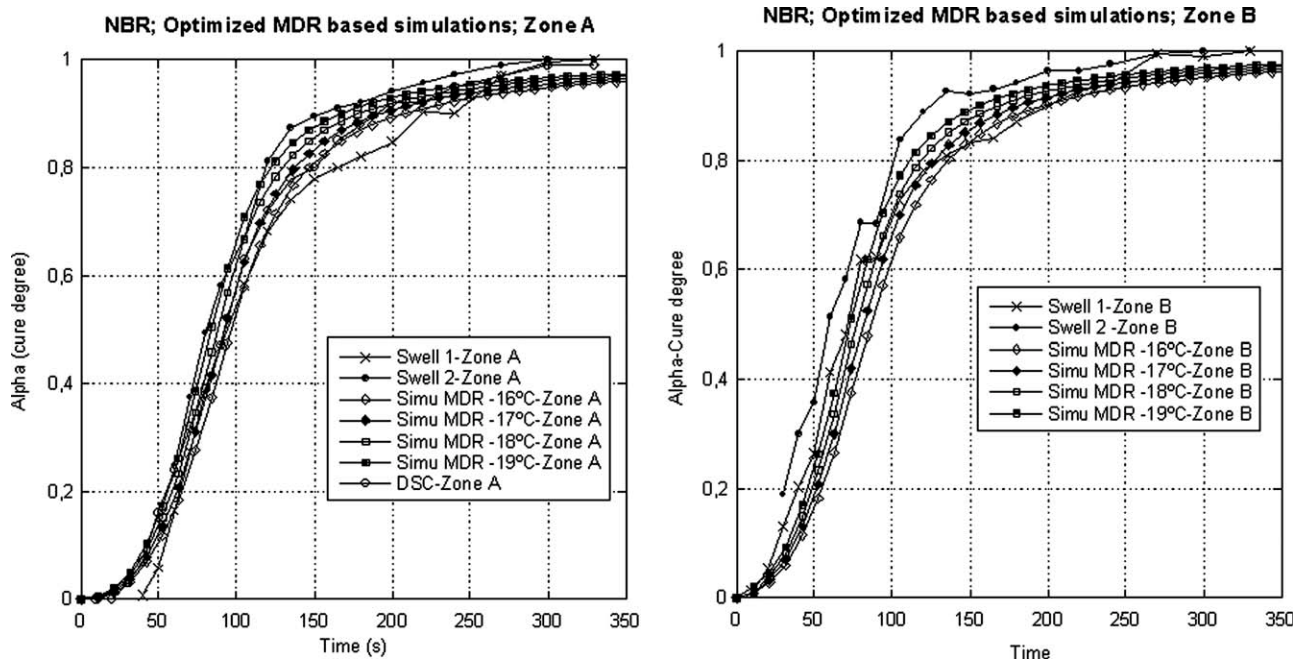

Figure 10 Predictions of the degree of cure for NBR after optimization (Moldflow). The material was characterized from MDR cure tests. The term "simu" indicates it is a simulation result curve.

simulations. The failure to achieve 100% cure profiles was attributed to the shape of the cure models themselves because they continued predicting a lower degree of cure at long times, and consequently, extremely long times were required to achieve a degree of cure attaining 100%.

Optimization of the Moldflow simulations

It was clearly observed that the cure kinetics predicted by the simulations were too slow. To speed up the cure process, the parameters of the cure model were recalculated by the assumption that tests were made at a lower temperature than that

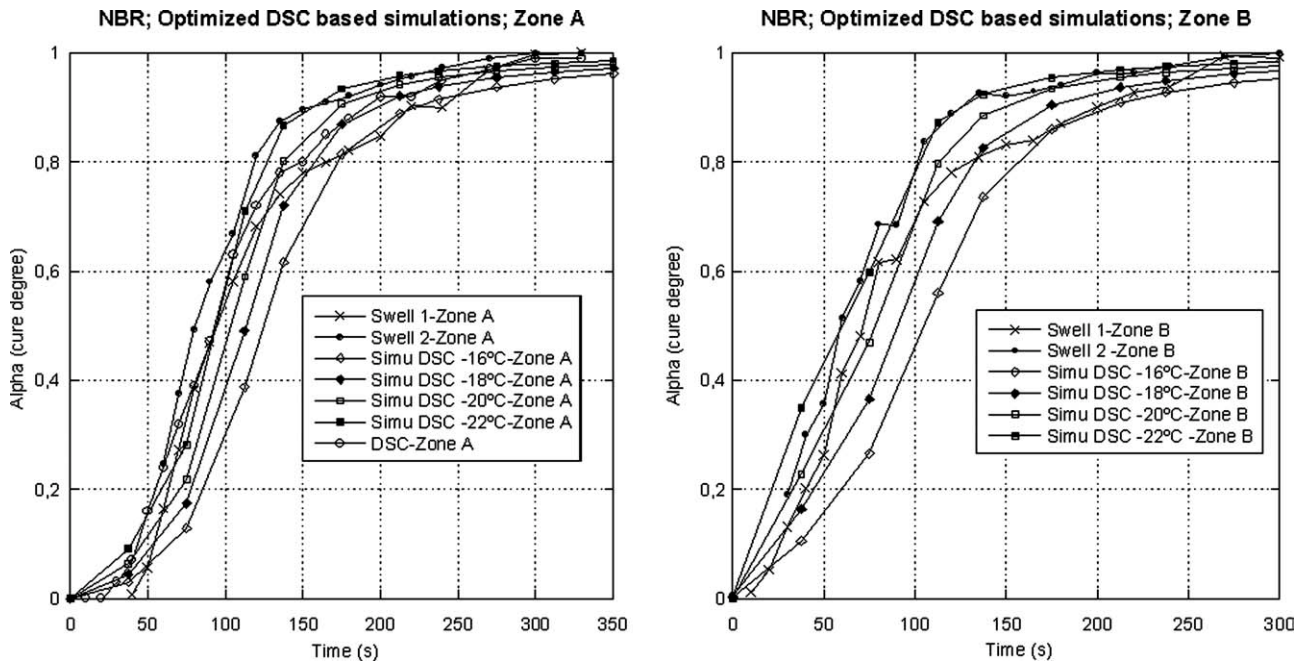

Figure 11 Predictions of the degree of cure for NBR after optimization (Moldflow). The material was characterized from DSC cure tests. The term "simu" indicates it is a simulation result curve.

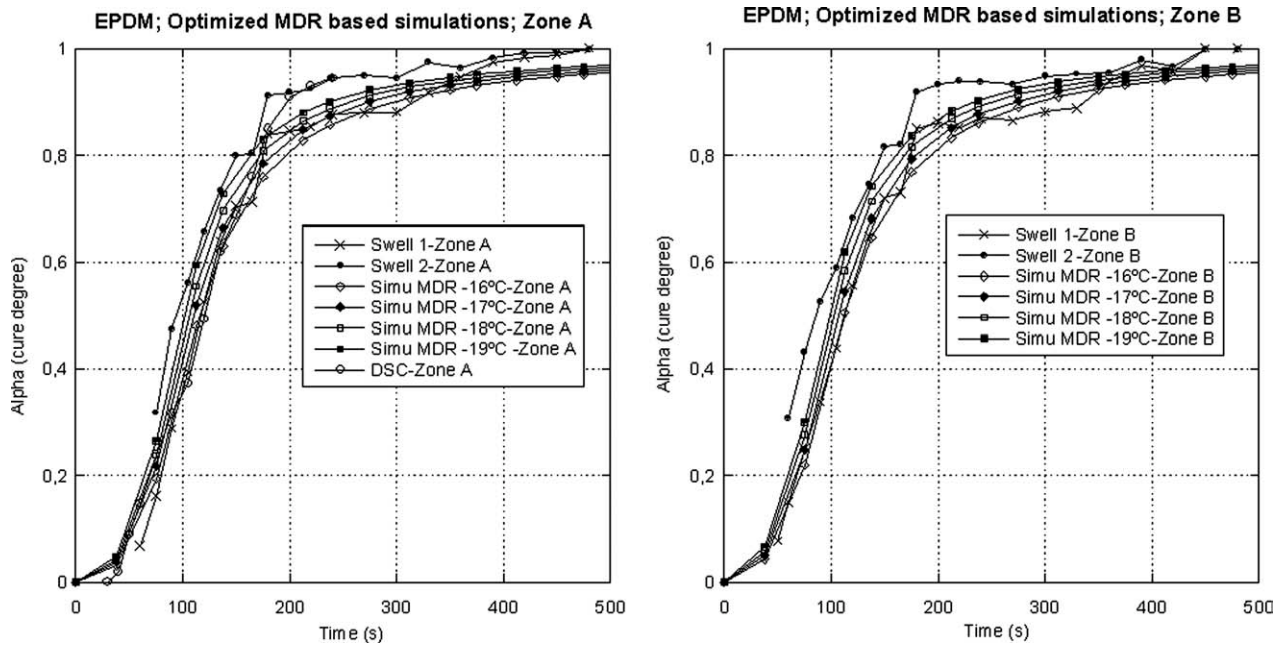

Figure 12 Predictions of the degree of cure for EPDM after optimization (Moldflow). The material was characterized from MDR cure tests. The term "simu" indicates it is a simulation result curve.

used in the experimental tests. For instance, by way of example, a cure curve from an MDR carried out at 180°C was regarded as a trace at 170°C for calculating the parameters of the Kamal model. Initially, a temperature reduction of 10% of the real mold temperature (about 160°C for both materials) was used first, and subsequently, we carried out further simulations by either decreasing or increasing the temperature to make the prediction of cure slower or faster, as was deemed appropriate. This methodology was applied to both the induction and cure kinetic models.

Experimental cure curves were compared with those that were obtained from the cure models in which systematic reductions in temperature were applied to calculate the cure model. The results of this comparison with the MDR and DSC are described in Figures 10–13.

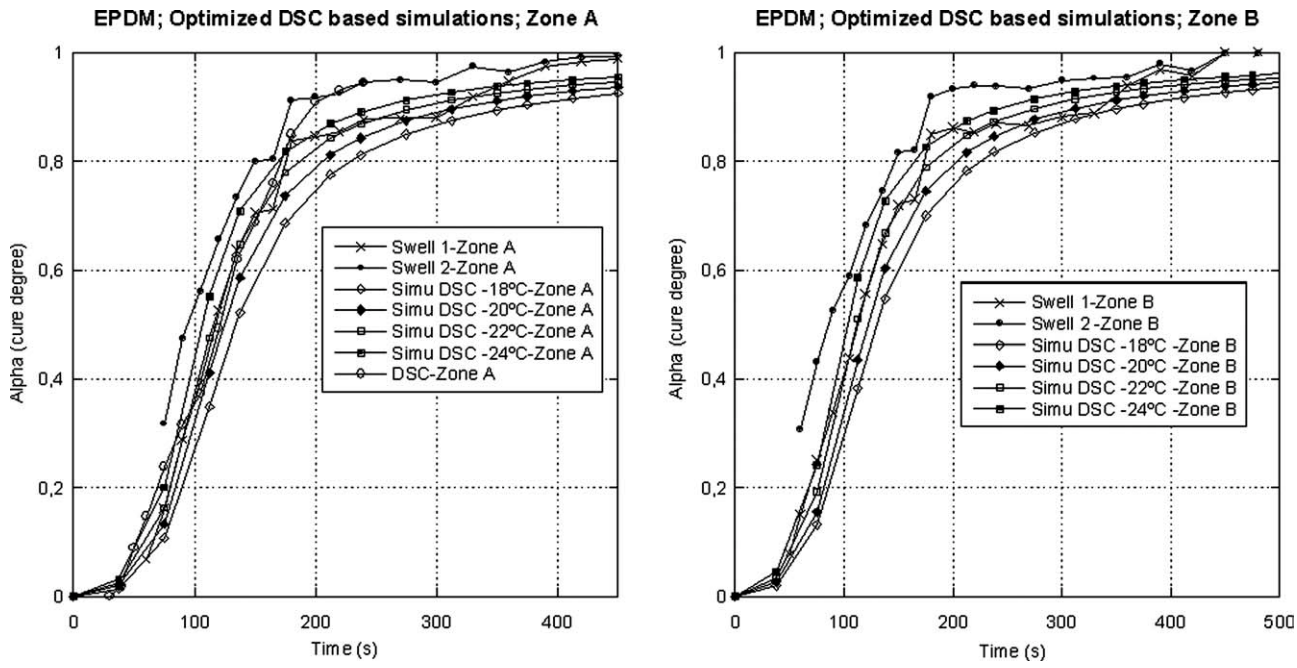

Figure 13 Predictions of the degree of cure for EPDM after optimization (Moldflow). The material was characterized from DSC cure tests. The term "simu" indicates it is a simulation result curve.

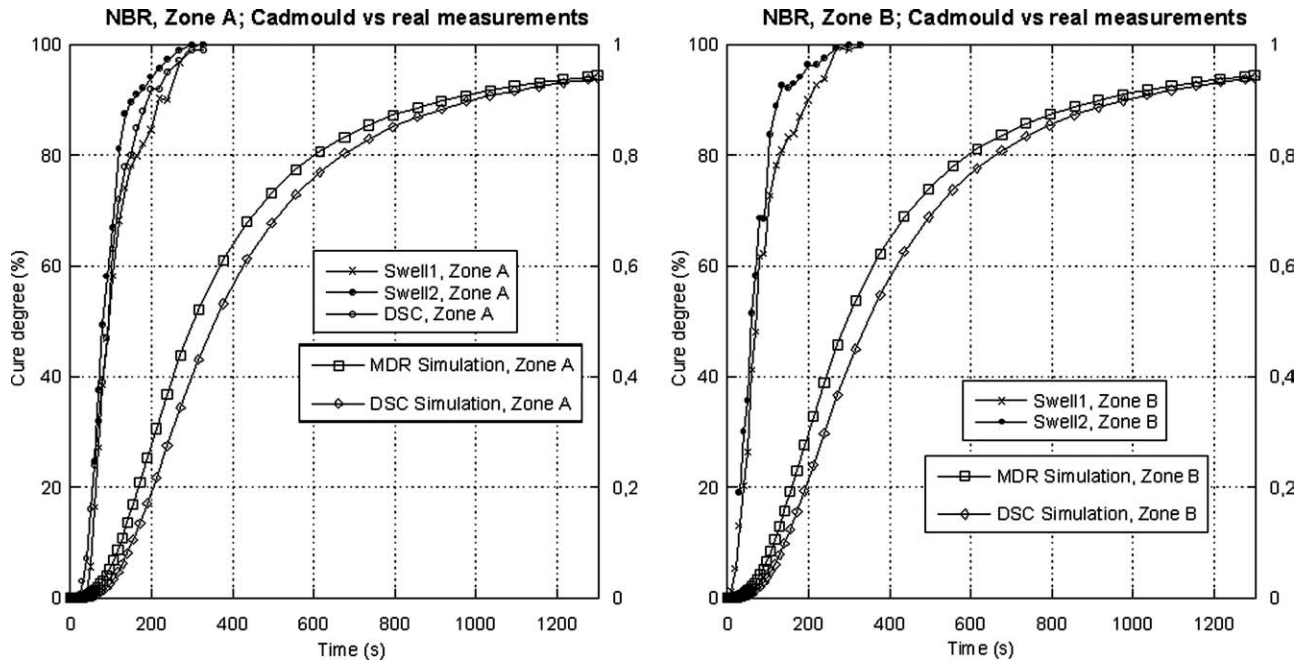

Figure 14 Comparison of the experimental and simulated (Cadmould) degrees of cure for NBR; for zones A and B. The term "simu" indicates it is a simulation result curve.

Regarding these results for the NBR formulation, the most promising results were obtained when a temperature reduction of 18°C was applied to recalculate the cure model parameters when MDR test data was used as a reference, whereas a reduction of 20°C was necessary when DSC test data were used. In contrast, for EPDM, reductions of 19 and 24°C were considered appropriate when MDR and DSC test data were used, respectively. The cure curve deemed appropriate was that which fell between the two experimental cure curves representing zones A and B, which were constructed from the data acquired from the swelling measurements. The temperature values showed that the cure model defined from the DSC data led to a slower curing than the one obtained from MDR, so higher temperatures were necessary to fit the data between the experimental cure curves.

Cadmould simulation results and comparison to the degree of cure measurements

A default cure time of 1300 s was set again for Cadmould's initial simulations. Two different parameters groups were used to define the induction[50] and cure models,[52,53] depending on the instrument from which the test data was attained: MDR or DSC (see Table V). Comparison of the experimental cure curves with those predicted by simulations using Cadmould are shown in Figures 14 and 15.

As was the case with the initial Moldflow simulations, the results from the Cadmould simulation showed slower cure profiles than those obtained in reality. Again, an unacceptably lengthy time was required to achieve a complete cure profile; thus, a faster rate of cure was considered necessary. For NBR, MDR was slightly faster than DSC, whereas for EPDM, MDR was faster than DSC at low degrees of cure.

Optimization of the Cadmould simulations

An analogous procedure to the one applied for Moldflow was used here to ensure that Cadmould produced a speedy cure prediction. Different temperature reductions were applied to calculate the new parameters for the cure model. Figures 16–19 depict the results of optimization carried out for both materials with both the MDR and DSC instruments.

In this case, for the NBR formulation, the most promising results were obtained when a temperature reduction of 22°C was applied to recalculate the cure model parameters when MDR test data was used as reference, whereas a reduction of 23°C was necessary when the DSC test data were used. In contrast, for EPDM, reductions of 20 and 23°C were considered appropriate when MDR and DSC test data were used, respectively. Again, the criteria used to select the most adequate curve were that which fell between the two experimental cure curves representing zones A and B, which were constructed from the data acquired from the swelling measurements. As in the case of the Moldflow simulations, the temperature values showed that the cure model defined from the DSC data led to a slower curing than the one obtained from MDR, so higher temperatures were necessary to fit the data between the experimental cure curves. We concluded that generally

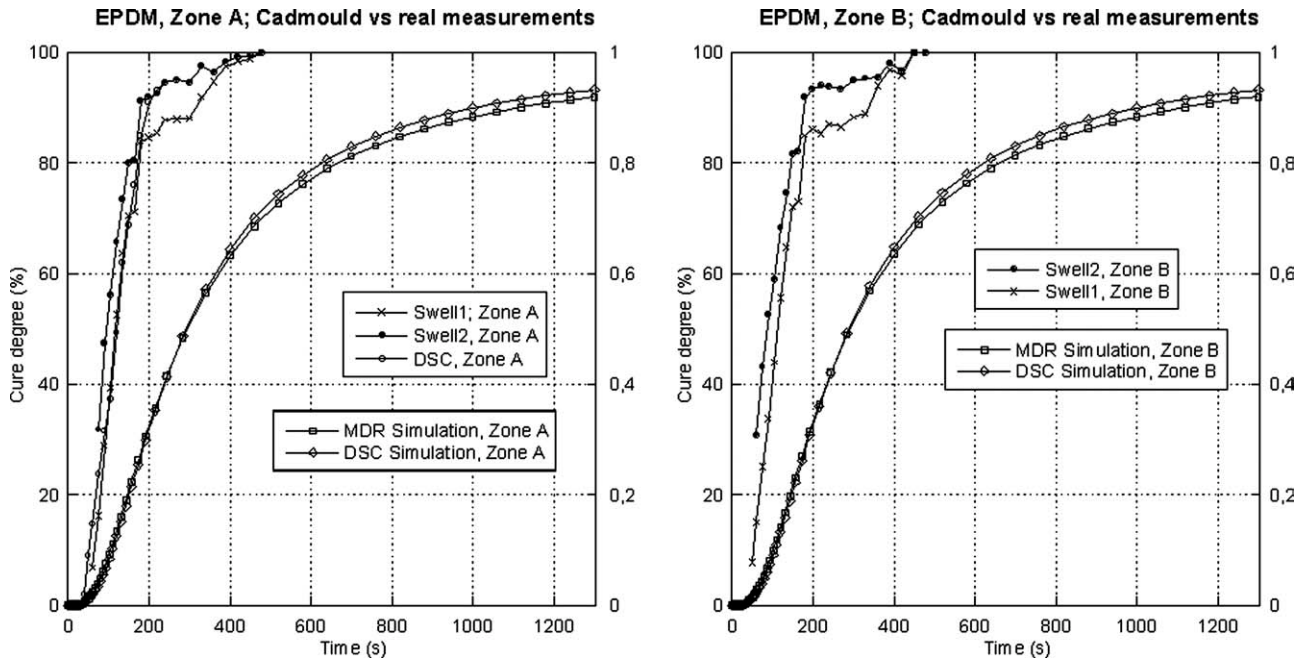

Figure 15 Comparison of the experimental and simulated (Cadmould) degrees of cure for EPDM for zones A and B. The term "simu" indicates it is a simulation result curve.

speaking, for the formulations used in this study, the cure kinetics described from the DSC data showed slower profiles than those defined with the MDR data.

Comparison between Moldflow and Cadmould for cure prediction

Induction models used to define the curing process were equal for both tools, but the cure kinetic model differed. Moldflow gave satisfactory results with the Kamal–Sourour model,[51] whereas Cadmould was effective with the Isayev model.[52,53] So, although the same cure test data (MDR or DSC) was used to define the material model in both tools, it is expected that they will give different cure predictions. Differences were also apparent in terms of defining the rheology model so the temperature profile calculated at the end of the mold-filling sequence would be different. These two factors, together with

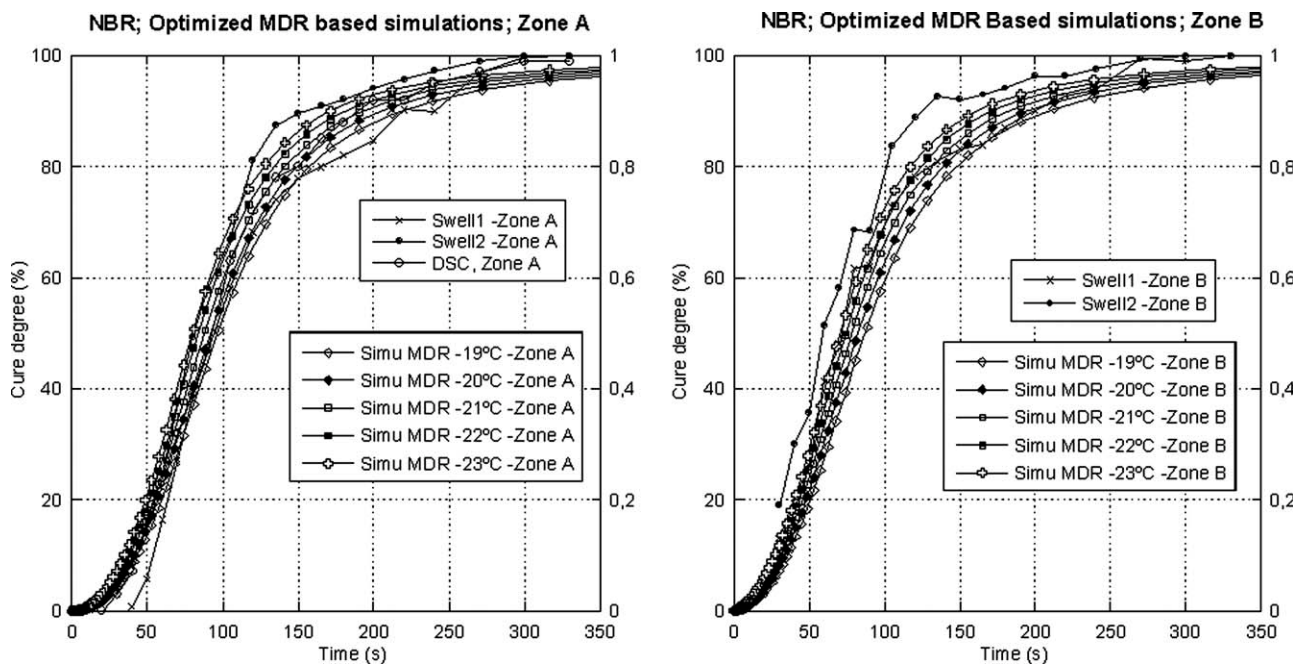

Figure 16 Predictions of the degree of cure for NBR after optimization (Cadmould). The material was characterized from MDR cure tests. The term "simu" indicates it is a simulation result curve.

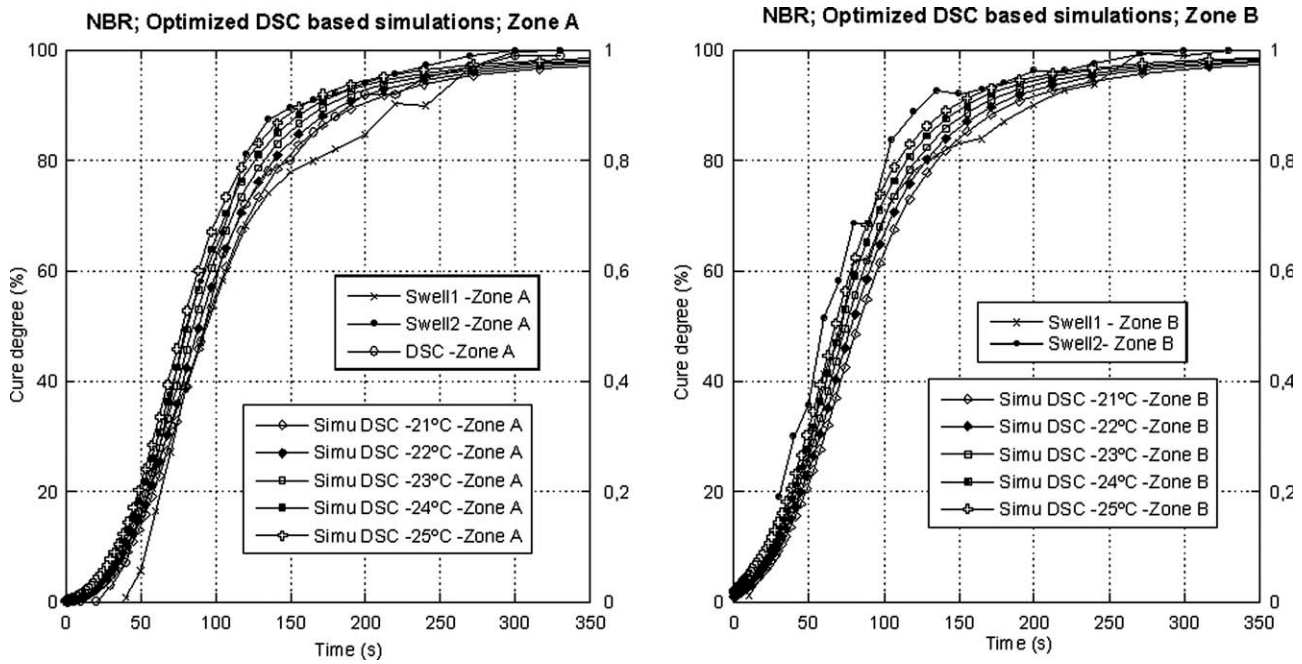

Figure 17 Predictions of the degree of cure for NBR after optimization (Cadmould). The material was characterized from DSC cure tests. The term "simu" indicates it is a simulation result curve.

the differences existing between both tools regarding the mathematics used to solve the problem, led to differences, even though the same process parameters were set on both. This was clearly evident when we considered the reduction in temperature to be applied to match the experimental cure profiles: Cadmould required a higher reduction than Moldflow. Thus, essentially, Moldflow predicted a faster cure under identical conditions. Notwithstanding, the differences among both simulation tools were quite similar.

For comparison purposes, Figure 20 compares the cure curves calculated with both packages after the optimum temperature reductions were applied to those obtained experimentally from swelling

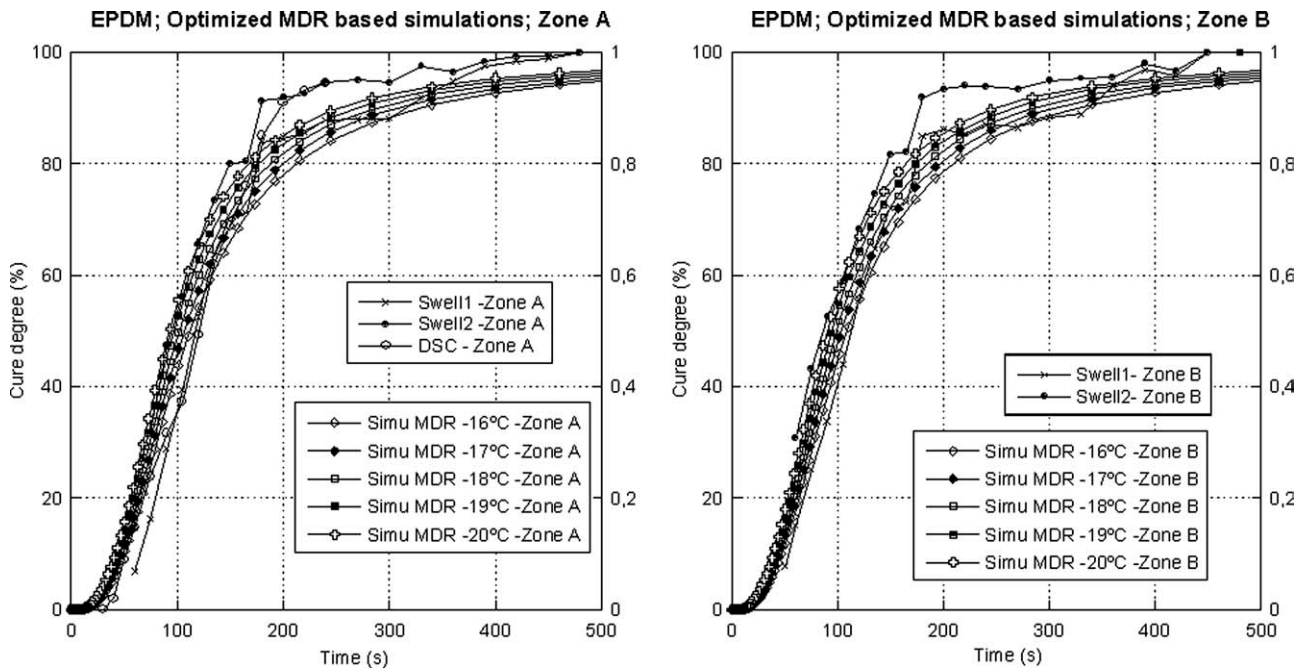

Figure 18 Predictions of the degree of cure for EPDM after optimization (Cadmould). The material was characterized from MDR cure tests. The term "simu" indicates it is a simulation result curve.

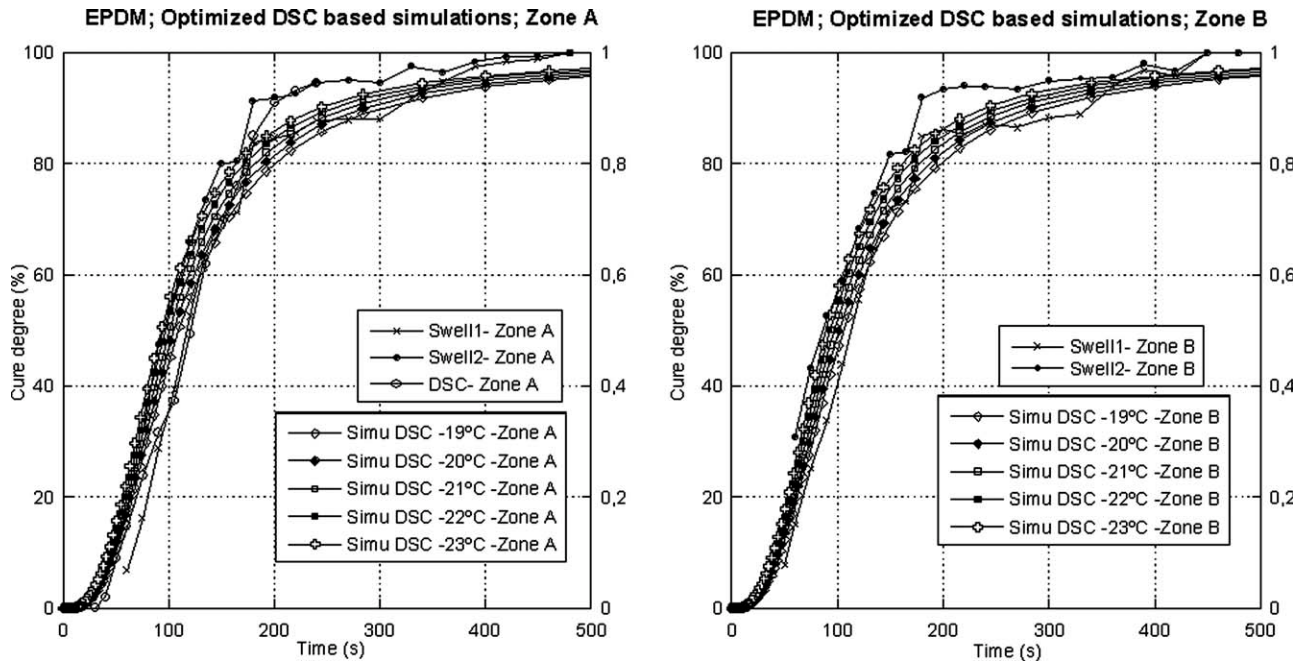

Figure 19 Predictions of the degree of cure for EPDM after optimization (Cadmould). The material was characterized from DSC cure tests. The term "simu" indicates it is a simulation result curve.

measurements. The cure model was defined with MDR test data.

DISCUSSION AND CONCLUSIONS

Two rubber formulations cured by peroxide were used in this study for injection-molding simulation purposes with Moldflow Reactive Molding and Cadmould 3D-F tools. A spiral-shaped part was injected into a mold with an REP V37 injection machine. Injection trials were carried out according to specific process parameters, and parts were produced with various cure times. Although temperatures were set for the injection unit and the mold, the real

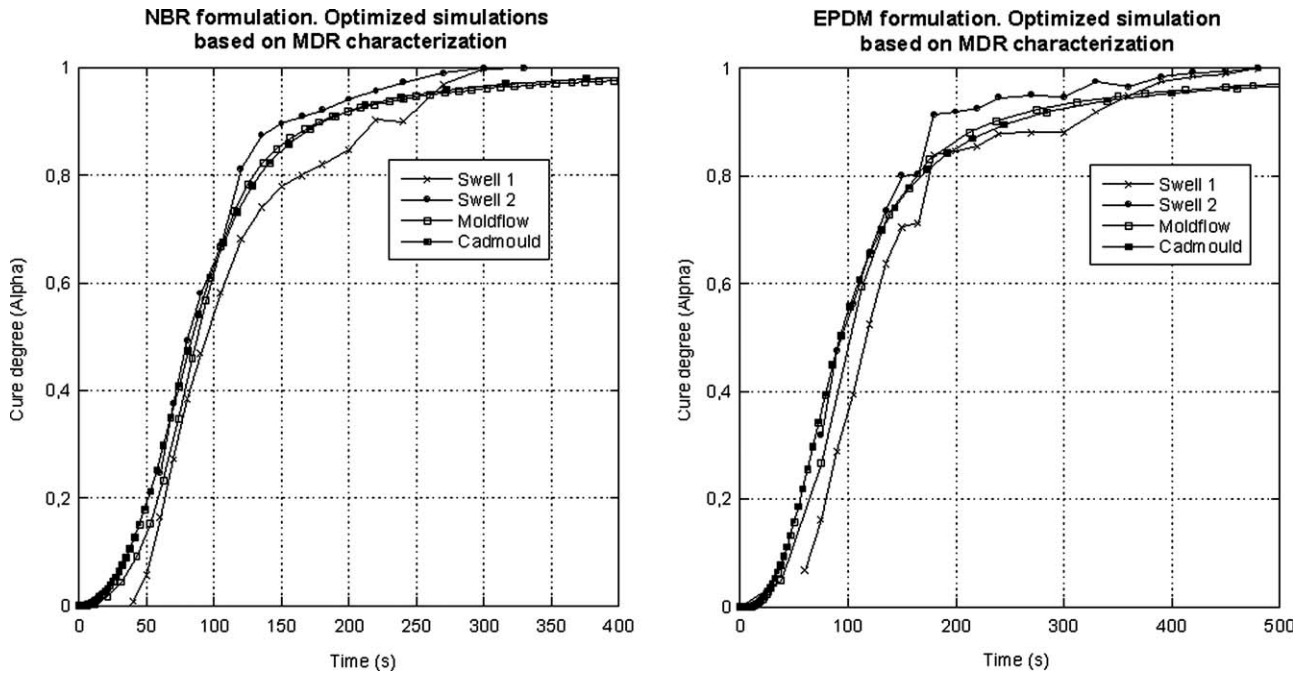

Figure 20 Comparison of the degrees of cure between the experimental data measured with the two swelling procedures and data calculated by the simulations produced by Moldflow and Cadmould (calculated from the MDR results) for both materials. The cure curves are those of intermediate temperatures.

temperatures differed from the set values. Temperature measurements were performed on the injection shoot and mold cavity to obtain real or actual values. These values were used in the simulation tools.

Parts cured to various extents were extracted from the mold, and the degrees of cure in two zones, A and B, were evaluated with three procedures, two of which were based on swelling measurements in appropriate solvents and the third of which was based on the measurement of residual exothermal heat of cure reaction with DSC. Each procedure produced its own characteristic value for the degree of cure; the results of the DSC method occupied a position that was intermediate between the two swelling procedures.

Simulations need to define the part in terms of an appropriate mesh and the process settings of the injection process. Rubber formulations need to be characterized in terms of the rheology and thermal and curing properties. The rheological behavior was characterized with an extrusion capillary rheometer, as is required for the reactive viscosity model[9] and the Carreau model.[11] The thermal properties measured included C_p, K, and thermal diffusivity measurements. Curing profiles were characterized with MDR and DSC isothermal tests. The results were fitted to the induction or scorch[50] and cure models.[51–53]

The initial simulations for both Moldflow and Cadmould were poor because predictions of the degree of cure were much lower than those defined with the two swelling and the DSC procedures. Models defined with DSC and MDR data gave similar results. Notwithstanding, small differences were apparent for NBR, where it was found that the MDR instrument gave a faster cure compared with that of DSC. The same trend was found for EPDM up to a specific level of cure; thereafter, opposite behavior was observed. To correlate the cure kinetics of simulated and actual trials, induction and cure kinetic model parameters were recalculated with a series of different temperature reductions until the results showed a reasonable fit to the experimental values for the degree of cure. We concluded that when we used DSC data as reference, a higher reduction was required to fit values to the degrees of cure in comparison to when we used MDR data. Differences in the cure models and the mathematical expressions applied to solve the cure solution appeared to show that Moldflow predicted faster cures than did Cadmould under identical conditions. Consequently, Cadmould required higher reductions in temperature to be invoked compared to Moldflow.

The authors thank London Metropolitan University for the supervision from A. S. Farid.

References

1. Arrillaga, A.; Zaldua, A. M.; Farid, A. S. Rubber Chem Technol 2009, 82, 62.
2. Arrillaga, A.; Zaldua, A. M.; Achurra, R. M.; Farid, A. S. Eur Polym J 2007, 43, 4783.
3. Blanchard, A. F. J Polym Sci Part B: Polym Lett 1971, 9, 509.
4. Blanchard, A. F.; Wootton, P. M. J Polym Sci 1959, 34, 627.
5. Osswald, T. A. Polymer Processing Simulations Trends; Madison Group-PPRC: Madison, WI, 2001.
6. Bagley, E. B. J Appl Phys 1957, 28, 624.
7. Bagley, E. B. Trans Soc Rheol 1961, 5, 355.
8. Rabinowitsch, B. Z Phys Chem A 1929, 145, 1.
9. MPI Reactive Moulding Manual. Autodesk Inc, Waltham, MA.
10. Grace Software (http://plasma-gate.weizmann.ac.il/Grace/); Free Software Foundation Inc, Boston, MA: 1991.
11. Carreau, P. J. Ph.D. Thesis; University of Wisconsin, Madison, 1968.
12. Williams, M. L.; Landel, R. F.; Ferry, J. F. J Am Chem Soc 1955, 77, 3701.
13. KaleidaGraph Software; Synergy Software (http://www.synergy.com/): Reading, PA, 2005.
14. Wunderlich, B. Thermal Analysis; Academic: San Diego, CA, 1990.
15. Varma-Nair, M.; Wunderlich, B. J Phys Chem 1991, 20, 349.
16. Agari, Y.; Veda, A.; Nagai, S. J Polym Sci Part B: Polym Phys 1995, 33, 33.
17. Malek, J. Thermochim Acta 1992, 200, 257.
18. Underwood, W. M.; Taylor, J. R. Polym Eng Sci 1978, 18, 558.
19. Lobo, H.; Cohen, C. Polym Eng Sci 1990, 30, 65.
20. Shojaei, A.; Ghaffarian, S. R.; Karimian, S. M. H. Compos Struct 2004, 65, 381.
21. Kline, D. E. J Appl Polym Sci 1994, 5, 191.
22. Fujino, J.-I.; Honda, T.; Yamashita, H. Heat Transfer Jpn Res 1997, 26, 435.
23. Poularet, B.; Probst, N. Kautsch Gummi Kunstst 1986, 39, 102.
24. Sombatsompop, N.; Wood, A. K. Polym Test 1997, 19, 206.
25. Yue, M.; Wood, A. K.; El-Rafey, E. J Appl Polym Sci Appl Polym Symp 1994, 55, 105.
26. Price, D. M.; Jarratt, M. Thermochim Acta 2002, 392–393, 231.
27. Thermal Conductivity; PerkinElmer Inc, San Jose, CA.
28. Sircar, A. K.; Wells, J. L. Rubber Chem Technol 1981, 55, 191.
29. Marcus, S. M.; Blaine, R. L. Thermal Conductivity of Polymers, Glasses and Ceramics by Modulated DSC; TA Instruments, Newcastle, DE, 1994.
30. Khanna, Y. P.; Taylor, T. J.; Chomyn, G. Polym Eng Sci 1988, 28, 1038.
31. Riesen, R. UserCom 2005, 22.
32. Camirand, C. P. Thermochim Acta 2004, 417, 1.
33. Ismat, A. I. Thermal Properties of Automotive Polymers II. Thermal Conductivity Measurements; SAE Report 2000–01-1320. Society of Automotive Engineer's World Congress, Detroit, MI, 2000.
34. Bafrnec, M.; Juma, M.; Toman, J.; Jurniová, J.; Kunma, A. Plast Rubber Compos 1999, 28, 482.
35. Juma, M.; Bafrnec, M. J Reinf Plast Compos 2000, 19, 1024.
36. Hayes, R. A. Rubber Chem Technol 1986, 59, 138.
37. Hands, D.; Horsfall, F. Rubber Chem Technol 1977, 50, 253.
38. Hands, D. In Handbook of Polymer Testing; Brown, R., Ed.; Marcel Dekker: New York, 1999; Chapter 24.
39. Hands, D. RubberWorld 1991, 1.
40. Gregory, I. H.; Muhr, A. H.; Imizan, A. B. J Rubber Res 1999, 2, 1.
41. Karam, S. Ph.D. Thesis, L'école Nationale Supérieure des Mines de Paris, 1995.
42. Fan, R. L.; Zhang, Y.; Huang, C.; Gong. P.; Zhang, Y. Rubber Chem Technol 2002, 75, 287.
43. Ding, R.; Leonov, A. I. J Appl Polym Sci 1996, 61, 455.

44. Brazier, D. W.; Nickel, G. H.; Szentgyorghyy, Z. Rubber Chem Technol 1980, 53, 160.
45. Brazier, D. W.; Nickel, G. H. Rubber Chem Technol 1975, 48, 26.
46. Coran, A. Y. Rubber Chem Technol 1964, 37, 689.
47. Ding, R.; Leonov, A. I.; Coran, A. Y. Rubber Chem Technol 1996, 69, 81.
48. Isayev, A. I.; Sobhanie, M.; Deng, J. S. Rubber Chem Technol 1988, 61, 906.
49. Han, I. S.; Chung, C. B.; Lee, J. W. Rubber Chem Technol 2000, 73, 101.
50. Claxton, W. E.; Liska, J. W. Rubber Age 1964, 9(5), 237.
51. Kamal, M. R.; Ryan, M. E. Polym Eng Sci 1980, 20, 859.
52. Isayev, A. I.; Deng, J. S. Rubber Chem Technol 1988, 61, 340.
53. Isayev, A. I.; Sobhanie, M.; Deng, J. S. Rubber Chem Technol 1988, 61, 906.
54. (a) Flory, P. J.; Rehner, J. J Chem Phys 1943, 11, 512; (b) Flory, P. J.; Rehner, J. J Chem Phys 1943, 11, 521.